Pergamon

SCIENCE DIRECT®

Tetrahedron 59 (2003) 8099–8105

TETRAHEDRON

Transition state analysis on regioselectivity in [2+2] photocycloaddition reactions of substituted 2-cyclohexenone with cycloalkenecarboxylates

Huda Izzat Omar,[a] Yuka Odo,[a] Yasuhiro Shigemitsu,[b] Tetsuro Shimo[a] and Kenichi Somekawa[a,*]

[a]*Department of Applied Chemistry and Chemical Engineering, Faculty of Engineering, Kagoshima University, 1-21-40 Kagoshima, Korimoto, Kagoshima 890-0065, Japan*
[b]*Industrial Technology Center of Nagasaki, Ikeda, Omura, Nagasaki 856-0026, Japan*

Received 14 May 2003; accepted 22 August 2003

Abstract—The experimental results of the triplet [2+2] photocycloaddition reactions of substituted 2-cyclohexenone **1** with cycloalkenylesters **2**, **3**, **4** have showed remarkable change in the regioselectivity of the products. The ht/hh product ratio increases with increment of the cycle-size. The FMO investigations in addition to the transition state analysis were used to rationalize such regioselectivity. The FMO method with their orbital coefficients and energies could not explain the reaction selectivity since these values of **2**–**4** showed tendency to form the hh adduct mainly. PM3, PM5, CIS/6-31G, and B3LYP/6-31G methods were used to locate the hh and ht transition states of the three reactions. As the potential energy barriers (TS1) on the first TS surface for the major products were lower than that for the minor products in most of the cases, the real ratio can be explained in terms of TS analysis. The recently improved PM5 and the B3LYP methods were more successful in this debate as partitioning the activation energy at the potential energy barriers into reactant deformation and the interaction (or repulsion) energies is easy and effective. The changes in the ht/hh ratio with the enlargement of the alkene ring size may be due to the increment of the repulsion energy and large changes in the deformation energy of the reactants. In the transition state structures the stabilities of the major products are thought to be due to the existence of some repulsion between the enone carbonyl and esters in the alkenylesters, and some hydrogen bonding between the reactants. The FMO and second transition state (TS2) energy on the biradical intermediates are also thought to play some role in controlling the product selectivity by lowering the closure energy of the biradicals according to the possibility of their overlapping.

1. Introduction

Photochemical [2+2] cycloadditions have been utilized to synthesize many kinds of important compounds.[1] Cycloaddition regioselectivity has remained a topic of great interest in this area.[2,3] The regiochemical preferences in cyclohexenone-alkene photoadditions have been nicely explained by using ab initio MO analysis of the first biradical producing step on the model reactions of triplet acrolein with alkenes.[3] The phenomenon associated with head-to-head vs head-to-tail adduct formation from other α,β-unsturated carbonyl cyclopentenones, however, has not been similarly addressed. The biradical trapping experiments conducted on those systems have led to the suggestion that the regioselectivity of these reactions is governed by the relative rates of biradical closure vs their return to starting materials by bond fragmentation.[4] These contrasting conclusions clearly demonstrate that the mechanism and source(s) of regiochemical control in excited state [2+2] photocycloadditions are still unresolved issues. Our teamwork has used successfully some FMO calculations to investigate the photocycloaddition reactions of pyrones, pyridones and cyclic enones.[5] The photochemical investigation process of enone–alkene systems will be continued by the transition state (TS) analysis.[6]

This study covers different computational methods that have been used to analyze the drastic photocycloaddition reactions of substituted 2-cyclohexenone (**1**) with cyclic alkenes **2**, **3**, and **4**. The experimental results are shown in Scheme 1.[7] The [2+2] photocycloaddition reactions of asymmetrical alkenes in its ground state (S) with the excited unsaturated ketone in its triplet state gave two regioisomers, hh- and ht-adducts. The hh/ht ratio usually depends on whether the alkene contains electron withdrawing or donating groups.[2] The mechanistic analysis of such reaction suggests a two-step mechanism involving the formation of a biradical intermediate. The cycloadduct ht/hh ratio of the

Keywords: cyclohexenone; cycloalkenecarboxylate; photocycloaddition; regioselectivity; transition state analysis; PM5; B3LYP/6-31G; deformation energy.
* Corresponding author. Tel.: +81-99-285-8330; fax: +81-99-285-8334; e-mail: some@apc.kagoshima-u.ac.jp

0040–4020/$ - see front matter © 2003 Published by Elsevier Ltd.
doi:10.1016/j.tet.2003.08.052

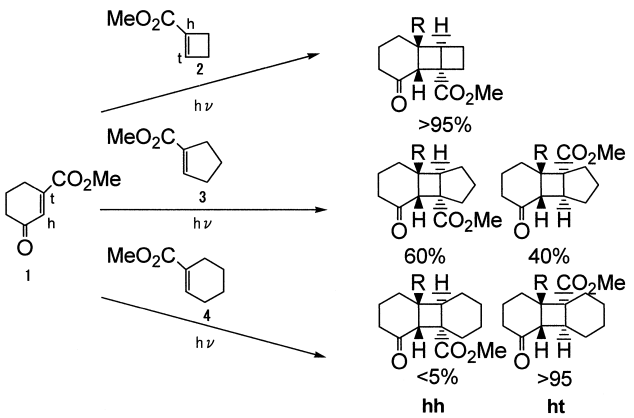

Scheme 1. Experimental regioselectivity on photocycloadditions of cyclohexenone **1** with cyclobutenylester **2**, cyclopentenylester **3** and cyclohexenylester **4**.

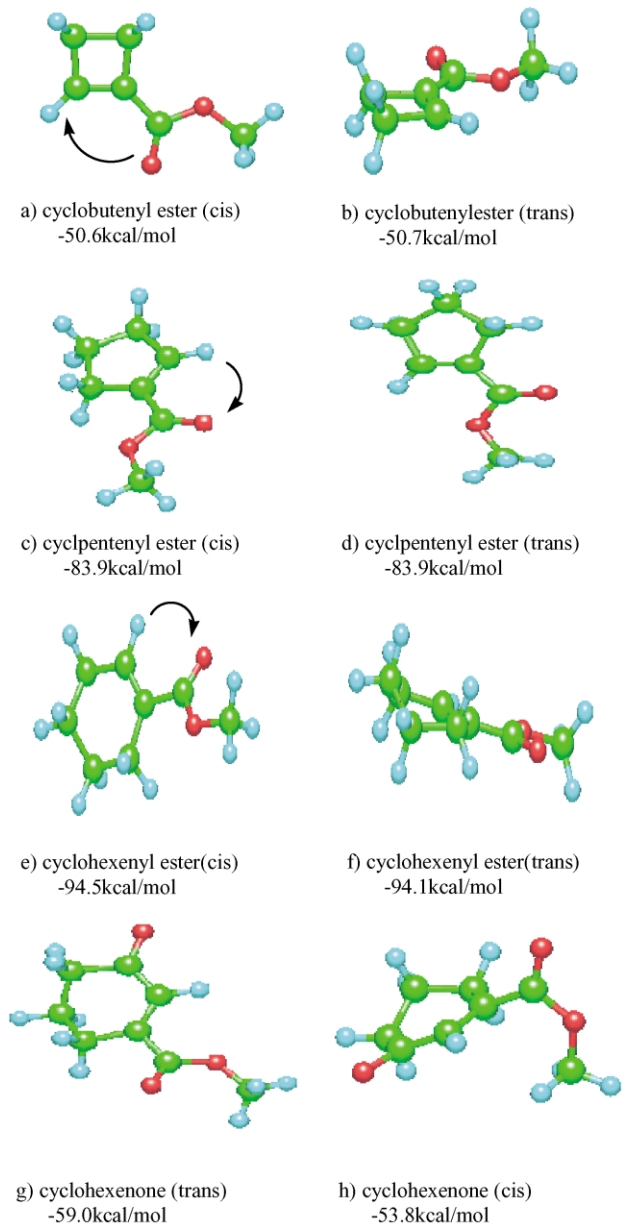

Figure 1. Reactant optimized geometry structures and heat of formations of enone triplet (**1**), and ground state alkenes (**2**, **3**, **4**) calculated by PM5 method.

reaction of **1** with **3** is 40/60, while the reactions with other cycloalkenylesters showed noticeable change in the ht/hh ratio. It is clear that this ratio decreases with increment of the alkene's cycle size.[7] Our aim is to find out the reason behind this drastic change in the product's selectivity using TS analysis in addition to the FMO analysis.[5] We thus carried out a theoretical study of these reactions, considering a triplet state enone and ground state cyclic alkenes.

2. Methodological and computational details

1. All geometry optimization and TS calculation at ground states and excited triplet states were performed using PM3[8] and PM5,[9] which are available in the molecular orbital package WinMOPAC3.5 by Fujitsu Ltd.[10]
2. The calculation was recalculated using the CIS,[11] B3LYP[12] and the standard 6-31G basis set in GAUSSIAN 98.[13] The single point and optimized geometry were introduced from PM5 calculations, as we had excellent results by the PM5 method for TS energy calculations on the stereoselectivity of the Diels–Alder reaction.[14] Energy minimum structures all had real frequencies and transition structures had only one imaginary frequency. The recently improved PM5 was more effective in explaining the results and discussion.

3. FMO analysis

The first way we can think of to rationalize reactivity and regioselectivity of the cycloaddition reactions is simply the FMO theory, which has led to some good explanation of enone–alkene photocycloaddition reactions.[5] We therefore studied the triplet and ground state geometries and orbital properties of enone **1** and olefins **2**, **3**, **4** as shown in Figures 1 and 2. The most stable conformer of the enone triplet is when the methoxycarbonyl group is in trans position with the ring double bond. Cycloesters have two conformers *cis* and *trans*, and the *cis* one has tendency to be more stable at the larger cycles. An inspection of the molecular orbitals in Figure 2 shows that the $LSOMO_{enone}-HOMO_{alkene}$ energy differences were smaller than those of the corresponding $HSOMO_{enone}-LUMO_{alkene}$. Consequently, the more effective frontier orbitals are the $LSOMO_{enone}-HOMO_{alkene}$, and the preferable adducts from the orbital interaction are inferred to be hh ones. The energy and coefficients of the ($LSOMO\text{-}1_{enone}$) level that has larger coefficients than LSOMOenone at the αβ position of **1** also suggest the hh adduct. Accordingly the differences in the products ratio (ht/hh) of **2**, **3** and **4**, cannot be explained using FMO analysis alone.

4. Transition state analysis

The photochemical [2+2]cycloadditions of cyclic enone to substituted alkenes start from attack of the excited triplet state of α,β-enone to the ground state alkenes.

The reaction passes the first transition state (TS1) and then

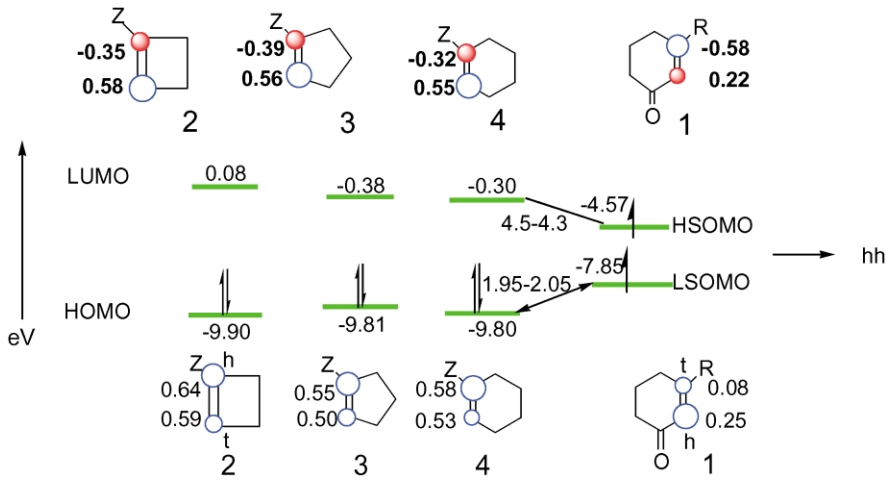

Figure 2. The FMO coefficients and energy levels (eV) for the enone triplet excited state (T1) and cycloalkenester (S0) by use of PM5 method.

involves the formation of biradical intermediates that, in turn, close to form the final hh or ht adducts after passing through the second transition state (TS2), which indicates a two-step mechanism. As mentioned before, the ratio of the ht/hh adduct is said to be dependent on the alkenes electron affinity,[3] such reasoning, however, are not applicable to these reactions of cyclohexenone with cycloalkenylesters (Scheme 1). We therefore, thought to use the TS1 analysis to see whether the ht/hh adduct ratio depends on the barrier height to the TS surface leading to formation of the biradical intermediate. The competition between the biradical closure to the products (TS2) with the partitioning to regenerate the ground state reactants (TS3) is also considered in this debate. It can be determined theoretically by TS2 and TS3 level investigation.

Semiempirical (PM3, PM5), DFT and ab initio methods were used to locate the transition states corresponding to the photochemical hh and ht adducts. Several transient conformers for each regioisomer were explored, and the most stable transient conformers were selected. The calculated TS1 values and the TS1 energy differences (hh-ht) calculated by kcal/mol with the experimental data are presented in Tables 1 and 2.[4] In the reaction of cyclobutenylester (**2**) the hh adduct is more stable by 0.8 kcal/mol than the corresponding ht adduct using the PM5 method, and by 0.4, 21.4 kcal/mol using the PM3 and CIS methods, and also 8.2, 0.4 kcal/mol by the B3LYP (single point) and B3LYP (optimized geometry) methods consequently. The more stable TS for the hh adduct and the smaller activation energy explains the hh selectivity. Moreover, the PM5 method reasonably explained the regioselectivity for the reaction of cyclopentenylester (**1**+**3**) and the reaction of cyclohexenylester (**1**+**4**). While

Table 1. First transition state energies (TS1) for the photoadditions of cycloalkenylester to cyclohexenone computed at different levels

Adduct hh/ht (exp%)	TS1				
	PM3 (kcal/mol)	PM5 (kcal/mol)	Ab initio CIS/6-31G//PM3 (a.u.)	B3LYP/6-31G//PM5 (a.u.)	B3LYP/6-31G[a] (a.u.)
1+2					
hh>95%	−102.1	−122.7	−914.30550	−919.99249	−920.02325
ht<5%	−101.7	−121.9	−914.27124	−919.97948	−920.02263
1+3					
hh=60%	−133.1	−154.6	−953.37044	−959.33601	−959.36864
ht=40%	−134.1	−153.9	−953.33958	−959.33336	−959.37103
1+4					
hh<5%	−138.4	−161.6	−992.38821	−998.63693	−998.68200
ht>95%	−141.4	−163.8	−992.37979	−998.65251	−998.69259

[a] Optimized geometry by B3LYP method.

Table 2. Calculated transition states energies differences (hh−ht)

Reaction	ΔE(hh−ht) (kcal/mol)					
	PM3	PM5	CIS/6-31G//PM3	B3LYP/6-31G//PM5	B3LYP/6-31G[a]	Exp.[b]
1+2	−0.4	−0.8	−21.4	−8.2	−0.4	≦−1.7
1+3	1.0	−0.7	−19.3	−1.6	1.5	−0.2
1+4	3.0	2.2	−5.3	9.7	6.6	≧1.7

[a] Optimized geometry by B3LYP method.
[b] The experimental results were calculated using Scheme 1 and Ref. 7.

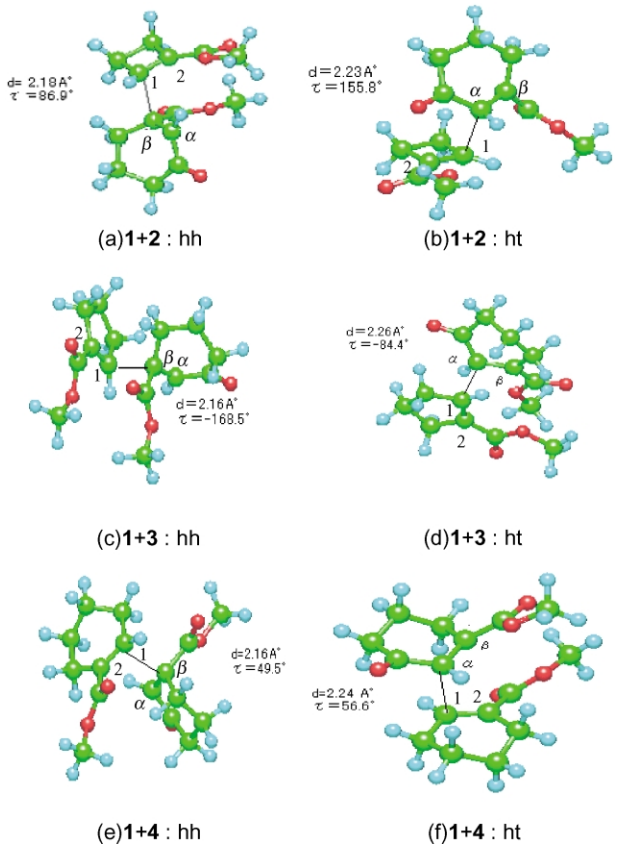

Figure 3. PM5 optimized transition state structures for the photoreactions of enone with cycloalkenyl esters. TS distances (d) are in Å, dihedral angles (τ) 1-2-α-β are in degrees.

PM3 method gave slightly poor results in explaining the cyclopentenylester reaction, where the TS energy for hh adduct was less stable than the TS for the ht adduct, which is not consistent with the experimental data. On the other hand, the CIS/6-31G method failed to explain the reaction selectivity of cyclohexenylester, since the TS energy barrier of the ht adduct was even 5.3 kcal/mol higher than that of the corresponding hh. These TS energy differences (hh−ht) arise from the balance between the reactants (triplet enone and ground state alkenes) and the transition state energies, which may depend on the method approximation. Transition states of optimized structures obtained by PM5, which gave good explanation for the reaction results, are shown in Figure 3. TS distances (d, Å) and dihedral angle 1-2-α-β (τ, °) are also presented. The TS distances of hh are shorter (2.16–2.18 Å) than those of ht (2.23–2.26 Å).

Potential energies for the whole reaction progress were located using the improved PM5 method. The energies of the biradicals, reversion of the biradicals, and cycloadduct formation are presented in Table 3. All second bond formation TS (TS2) was smaller than the TS (TS3) of the biradical reversion to products. The potential energy for the major products was also lower than those for minor products.

The calculation for the reaction of both cis and trans cyclopentylester (Fig. 1(c) and (d)) with the enone were done using the above methods. The *cis* structure gave better results than the *trans* one. Thus, we may consider that the *cis* structure is the real structure for the cyclopentylester.

Table 3. Calculated potential energies for the whole reaction progress using PM5 method of calculations

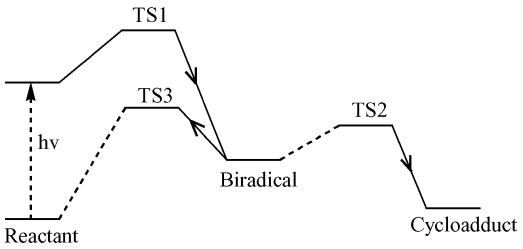

Reaction	Potential energies (kcal/mol)				
	TS1	Biradical	TS2	TS3	Cycloadduct
1+2					
hh	−122.7	−163.1	−162.1	−146.2	−208.1
ht	−121.9	−167.9	−163.1	−150.6	−205.7
1+3					
hh	−154.6	−190.4	−187.4	−176.8	−232.2
ht	−153.9	−194.5	−190.6	−181.1	−230.1
1+4					
hh	−161.6	−193.7	−179.5	−180.9	−211.9
ht	−163.8	−199.4	−196.1	−189.0	−235.3

In an effort to explain the increment of the ht/hh ratio with increment of the cycle size, we have estimated the deformation energies (E^{def}) of the alkenes and enones using the B3LYP/6-31G single point calculation on PM5 method. This was the first deformation analysis for the photochemical reactions. These are the energies required to deform the structures into their transition state geometries. Such calculations were shown in explanations of the facial selectivity in the Diels–Alder reaction.[15] Consequently, we have calculated the energy resulted from the interaction which was some repulsion between the alkenes and the enones ($\Delta E^{\text{int}}>0$) and it can be calculated as follows: $\Delta E^{\text{int}}=E^{\text{TS}}-(E^{\text{def-enone}}+E^{\text{def-alkene}})$ (E^{TS} were taken from Table 1). These energies are presented in Tables 4 and 5. We found that the interaction energy (which was repulsion) in the ht reactions is decreasing with increment of the cycle size of the alkenes and increases in the hh reactions through the enlargement of the cycle size of the alkenes, in addition we found that there is a slight attraction in the ht structure of the cyclohexenylester estimated by −0.04 kcal/mol (Table 4). Moreover, $\Delta E^{\text{def-hf}}$ of the enone sharply increases with the increment of the alkenes ring in the hh reactions, and sharply decrease in the ht reactions. For example the $\Delta E^{\text{def-hf}}$ is 3.2 kcal/mol in the hh transition structure for **1+2** reaction, while it is 8.1 kcal/mol in the hh transition structures for **1+4** reaction. This may be due to the different nature of interaction between the enones and the different alkene ring sizes. The $\Delta E^{\text{def-hf}}$ of the alkenes increases in all cases, almost in the same amount (Table 5). These effects are thought to be the main cause of the drastic change of the hh/ht ratio with the increment of the alkenes cycle size.

The more stable TS's are attributable to the existence of hydrogen bonding between the enone oxygen and the alkene protons. Actually, the hydrogen bonding existed in all TS structures. It was more obvious in the more stable TS's since the distance between the hydrogen and the oxygen is shorter than that for the less stable TS (Fig. 4). This can be seen in

Table 4. The interaction energy calculated from TS energy and total deformation energy introduced from B3LYP/6-31G//PM5 method

Reactant	hh			ht		
	E^{TSa}	E^{def}	ΔE^{intb}	E^{TS}	E^{def}	ΔE^{int}
1+2	−919.9925		3.1	−919.97947		0.9
Alkene		−536.27388			−536.25483	
Enone		−383.72393			−383.72602	
1+3	−959.33601		5.2	−959.33336		0.5
Alkene		−536.27362			−536.26062	
Enone		−423.07086			−423.07354	
1+4	−998.63693		3.9	−998.65251		−0.04
Alkene		−536.26605			−536.27327	
Enone		−462.37716			−462.37916	

ΔE values are in kcal/mol, others in a.u.
[a] E^{TS} data are taken from Table 1.
[b] $\Delta E^{int}=E^{TS}-(E^{def\text{-}enone}+E^{def\text{-}alkene})$.

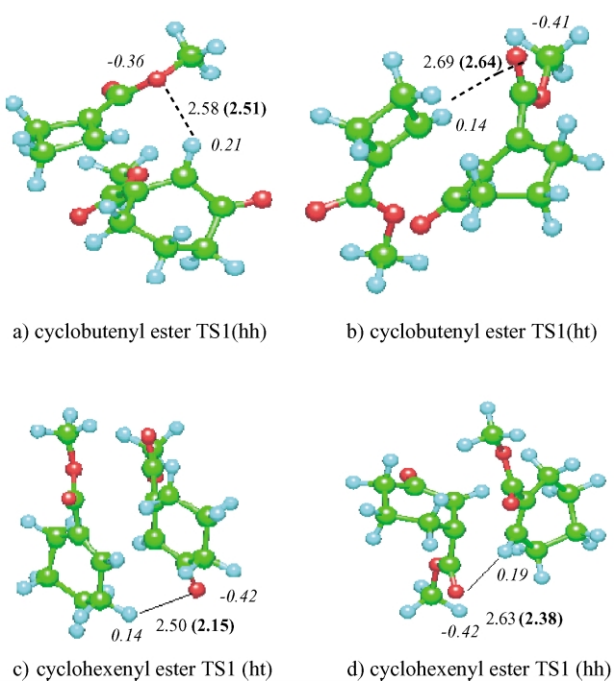

Figure 4. TS stabilities in the major products due to the existence of hydrogen bonding. Distances in all TS structures are presented by PM5 method and B3LYP/6-31G (parenthesis). Italic numbers are net atomic charges on the hydrogens and oxygens.

the cyclohexenylester reaction. The distance between the carbonyl and the hydrogen was around 2.5 Å by PM5 and 2.15 Å by B3LYP (optimized geometry) for the stable TS ht adduct, but it was longer for the less stable hh TS structure, as shown in Fig. 4(d).

As long as these reactions involve the biradical formation, it is worth considering the biradical role in controlling the reaction's selectivity. We tried to use again the FMO calculations, this time at the biradical intermediates to examine the tendency of the biradical to form the cycloadduct, or to break down to regenerate the starting reactants. We found that the orbital on the two radical ends plays a significant role in determining the product's selectivity. Table 6 shows the involved orbital kind and coefficients at the biradical's ends. For the first reaction **1+2**, the FMO for hh and ht biradicals were investigated and it was revealed that the hh biradical showed high tendency to form the cycloadducts, since the two radical ends in LSOMO and HSOMO bear p_z orbital of the biggest coefficients, which allow the larger overlapping between these orbitals. On the contrary, the ht biradical showed lesser tendency for bonding. The above results can also be applied for the **1+4** reaction, but in this case the ht biradical tends to form the cycloadduct, which is consistent with experimental results. Figure 5 presents the real orbitals obtained by the PM5 method. This phenomenon can be seen in the relatively lower TS2 (−199.4 kcal/mol in Table 3)

Table 5. Changes of the deformation energy with increment of alkene cycle-size calculated by B3LYP/6-31G//PM5 method

Reactant	hf[a]	hh		ht	
		E^{def}	$\Delta E^{def\text{-}hf}$	E^{def}	$E^{def\text{-}hf}$
1+2					
Enone(Triplet)	−536.27900	−536.27388	3.2	−536.25483	15.1
Cyclobutenyl ester	−383.72982	−383.72393	3.6	−383.72602	2.4
1+3					
Enone(Triplet)	−536.27900	−536.27362	3.4	−536.26062	11.5
Cyclopentenyl ester	−423.07771	−423.07086	4.3	−423.07354	2.6
1+4					
Enone(Triplet)	−536.27900	−536.26606	8.1	−536.27327	3.6
Cyclohexenyl ester	−462.38649	−462.37716	5.8	−462.37916	4.6

ΔE values are in kcal/mol, others in a.u.
[a] Heat of formations for the reactants.

Table 6. Biradicals FMO and the coefficients involved in second bond formation

Biradical	FMO					
	Position	(Orbital coeff.) hh		Position	(Orbital coeff.)ht	
		LSOMO	HSOMO		LSOMO	HSOMO
1+2						
	α	**p_z=0.71**	**p_z=−0.15**	β	p_z=0.64	p_z=0.52
	2	**p_z=0.18**	**p_z=0.80**	2	p_y=0.5	p_y=−0.59
1+3						
	α	p_z=0.72	p_z=0.35	β	p_z=0.68	p_z=0.49
	2	p_y=0.3	p_y=−0.6	2	p_y=0.47	p_y=−0.63
1+4						
	α	p_z=0.76	p_z=−0.19	β	**p_z=0.71**	**p_z=0.41**
	2	p_y=0.15	p_y=0.62	2	**p_z=0.31**	**p_z=0.61**

Bold type stands for the high tendency of bond formation from Figure 5.

and the smaller ΔE_{TS2} (2.7(−196.1+199.4) kcal/mol) at the ht reaction in Table 3.

5. Conclusion

In this research we used various levels of calculations to investigate the drastic change in the regioselectivity of the photocycloaddition reactions of cyclohexenone **1** with cycloalkenylesters **2**, **3** and **4**. FMO investigation for the triplet state reactions did not give reasonable justification for the selectivity. TS analysis showed good explanation for the selectivity preference since the TS energy barriers for the major products were lower than that for the minor products. TS analysis by the PM5 and B3LYP methods showed that the regioselectivity alteration is mainly caused from the first transition state (TS1) energy differences. Moreover, the deformation energies of the alkenes are believed to play a main role in controlling the reaction products. It was found that the $\Delta E^{\text{def-hf}}$ of the enone sharply increases with the increment of the alkenes ring in the hh reactions, and sharply decrease in the ht reactions. This may come from some repulsion between the enone carbonyl and esters in the alkenylesters. The TS stabilities are attributed to the existence of some hydrogen bonding between the reactants caused by the shorter distance. The biradical intermediate FMO and second transition state (TS2) energy difference are also thought to play some role in controlling the reaction selectivity.

References

1. (a) Demuth, M.; Mikhail, G. *Synthesis* **1989**, 145. (b) Keukeleire, D. D.; He, Shu.-L. *Chem. Rev.* **1993**, *93*, 145.

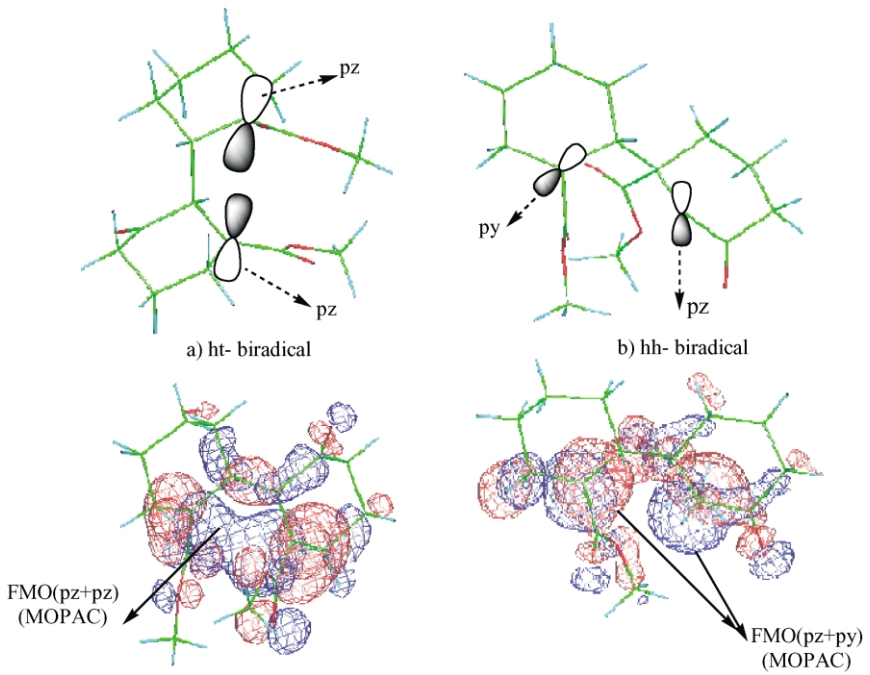

Figure 5. The biradical FMO effect on the formation of the cycloadducts. FMO for the **1+4** reaction represented by MOPAC program. (a) The larger ht biradical FMO interaction. (b) the smaller hh biradical FMO interaction.

2. (a) Schuster, D. I. *Chem. Rev.* **1993**, *93*, 3. (b) Andrew, D.; Hastings, D. J.; Weedon, A. C. *J. Am. Chem. Soc.* **1994**, *116*, 10870.
3. Broeker, J. L.; Eksterowicz, J. E.; Belk, A. J.; Houk, K. N. *J. Am. Chem. Soc.* **1995**, *117*, 1847.
4. (a) Maradyn, D. J.; Weedon, A. C. *Tetrahedron Lett.* **1994**, *35*, 8107. (b) Andrew, D.; Weedon, A. C. *J. Am. Chem. Soc.* **1995**, *117*, 5647.
5. (a) Somekawa, K.; Shimo, T.; Suishu, T. *Bull. Chem. Soc. Jpn* **1992**, *65*, 354. (b) Suishu, T.; Shimo, T.; Somekawa, K. *Tetrahedron* **1997**, *53*, 3545. (c) Suishu, T.; Obata, T.; Shimo, T.; Somekawa, K. *Nippon Kagaku Kaishi* **2000**, 167.
6. Shimo, T.; Uezono, T.; Obata, T.; Yasutake, M.; Shinmyouzu, T.; Somekawa, K. *Tetrahedron* **2002**, *58*, 6111.
7. Lange, G. L.; Organ, M. G.; Lee, M. *Tetrahedron Lett.* **1990**, *31*, 4689.
8. Stewart, J. J. P. *MOPAC 97*; Fujitsu Ltd: Tokyo, Japan, 1998.
9. Stewart, J. J. P. *Int. J. Quant. Chem.* **1996**, *58*, 133.
10. Stewart, J. J. P. *Win MOPAC V 3.5*; Fujitsu Ltd: Tokoyo, Japan, 2001.
11. Foresman, J. B.; Head-Gordon, M.; Pople, J. A.; Frisch, M. J. *J. Phys. Chem.* **1992**, *96*, 135.
12. (a) Becke, A. D. *J. Chem. Phys.* **1993**, *98*, 5648. (b) Lee, C.; Yang, W.; Parr, R. G. *Phys. Rev. B* **1988**, *37*, 785.
13. Frisch, A.; Frisch, M. J. *Gaussian 98*; Gaussian, Inc.: Pittsburgh, PA, 1998.
14. Kiri, S.; Odo, Y.; Shimo, T.; Somekawa, K. Society of Computer Chemistry, Jpn, Spring Meeting, Abst. 2p05, 2003.
15. Xidos, J. D.; Poirier, R. A.; Pye, C. C.; Burnell, D. J. *J. Org. Chem.* **1998**, *63*, 105.